





Publication Year	2021
Acceptance in OA @INAF	2023-02-01T13:17:22Z
Title	Test plan of the BEaTriX paraboloidal mirror at PANTER
Authors	SPIGA, Daniele; SALMASO, Bianca; BASSO, Stefano; SIRONI, GIORGIA; GHIGO, Mauro; et al.
Handle	http://hdl.handle.net/20.500.12386/33099
Number	INAF-OAB internal report 2021/02

 	Test plan of the BEaTriX paraboloidal mirror at PANTER				
Code: 02/2021	OAB Technical Report	Issue: 1	1	Class	Page: 1 / 18

Advanced Telescope for High-Energy Astrophysics (ATHENA)

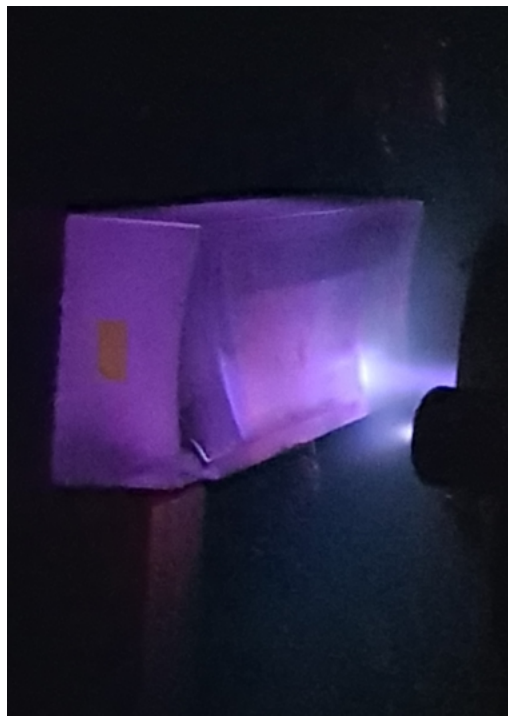
BEaTriX, the Beam Expander Testing X-ray facility



Test plan of the BEaTriX paraboloidal mirror at PANTER

Technical note by

***D. Spiga, B. Salmaso, S. Basso, G. Sironi, M. Ghigo, G. Vecchi,
V. Cotroneo, G. Pareschi, G. Tagliaferri (INAF/OAB)***



The BEaTriX collimating mirror under IBF, during a figuring run with argon ions.



Istituto Nazionale di Astrofisica (INAF)

Via del Parco Mellini, 00100 Roma, Italy

Osservatorio Astronomico di Brera (OAB)

Via Brera 28, 20121 Milano, Italy

Via E. Bianchi 46, 23807 Merate, Italy



 	Test plan of the BEaTriX paraboloidal mirror at PANTER				
Code: 02/2021	OAB Technical Report	Issue: 1	1	Class	Page: 2 / 18

Contents

Reference documents	2
Acronyms	3
1. Scope of the document	4
2. Preliminary analysis	5
2.1. Mirror geometry	5
2.2. Mirror metrology.....	5
2.2.1. Mirror profile.....	5
2.2.2. Mirror roughness.....	6
2.3. Mirror setup at PANTER	8
3. Test plan at PANTER, before coating	9
3.1. Tests in diverging beam at 1.49 keV.....	9
3.1.1. Initial alignment	9
3.1.2. Alignment in X-rays and best focus search.....	9
3.1.3. Measurement in the best focus	13
3.1.4. Measurement in intra-focus position.....	14
3.2. Measurement in parallel beam at 1.49 keV.....	15
4. Test plan at PANTER, after coating	16
5. Conclusions	18



Reference documents

- [RD1]. B. Salmaso, S. Basso, E. Giro, D. Spiga, G. Sironi, et al., "BEaTriX - the Beam Expander Testing X-Ray facility for testing ATHENA's SPO modules: progress in the realization," Proc. SPIE 11119, 111190N (2019)
- [RD2]. D. Spiga, B. Salmaso, M. Bavdaz, et al., "Optical simulations for the laboratory-based expanded and collimated x-ray beam facility BEaTriX," Proc. SPIE, 11110, 111100E (2019)
- [RD3]. Vecchi, G.; Salmaso, B.; Basso, S.; Sironi, G.; Ghigo, M.; Spiga, D.; Giro, E.; Pareschi, G.; Tagliaferri, G., "BEaTriX, the Beam Expander Testing X-ray facility for testing ATHENA's SPO modules: the collimating mirror," Proc. of the SPIE, Vol. 11119, 111191J (2019)
- [RD4]. M. Ghigo, S. Cornelli, R. Canestrari, D. Garegnani, "Development of a large ion beam figuring facility for correction of optics up to 1.7 m diameter," Proc. of SPIE 7426, 742611 (2009)
- [RD5]. Sironi, G., Citterio, O., Pareschi, G., Negri, B., Ritucci, A., Subranni, R., et al., "MPR: innovative 3D free-form optics profilometer," Proc. of the SPIE, Volume 8147, id. 814718 (2011)
- [RD6]. D. Spiga, B. Salmaso, G. Vecchi, "Coating samples for the BEaTriX mirrors: surface roughness analysis," INAF/OAB internal report 01/2021
- [RD7]. Salmaso, B., Spiga, D., "The BEaTriX parabolic mirror: manufacturing tolerances and expected results in UV and X-ray illumination," INAF/OAB technical report 05/2018
- [RD8]. Raimondi L., Spiga D., "Mirrors for X-ray telescopes: Fresnel diffraction-based computation of Point Spread Functions from metrology," Astronomy & Astrophysics, Volume 573, id. A22 (2015)
- [RD9]. D. Spiga, D. Cocco, C. L. Hardin, D. S. Morton, M. L. Ng, "Simulating the optical performances of the LCLS bendable mirrors using a 2D physical optics approach," Proc. of SPIE, Vol. 10699, 106993N (2018)
- [RD10]. Spiga, D.; Basso, S.; Bavdaz, M.; Burwitz, V., et al., "Profile reconstruction of grazing-incidence x-ray mirrors from intra-focal x-ray full imaging," Proc. of the SPIE, Vol. 8861, 88611F (2013)

 	Test plan of the BEaTriX paraboloidal mirror at PANTER					
Code: 02/2021	OAB Technical Report	Issue: 1	1	Class		Page: 3 / 18

Acronyms

ATHENA	Advanced Telescope for High-Energy Astrophysics
BEaTriX	Beam Expander Testing X-ray facility
CMM	Coordinate Measuring Machine
EA	Effective Area
ESA	European Space Agency
FFT	Fast Fourier Transform
HEW	Half Energy Width
IBF	Ion Beam Figuring
INAF	Istituto Nazionale di Astrofisica
MFT	Micro Finish Topographer
MPE	Max Planck Institut fur Extraterrestrische Physik
OAB	Osservatorio Astronomico di Brera
PSD	Power Spectral Density
PSF	Point Spread Function
RoC	Radius of Curvature
ZP	Zone Plate

 	Test plan of the BEaTriX paraboloidal mirror at PANTER				
Code: 02/2021	OAB Technical Report	Issue: 1	1	Class	Page: 4 / 18

1. Scope of the document

Scope of this technical note is the definition of a test plan for the X-ray characterization campaign of the BEaTriX paraboloidal mirror [RD1] at PANTER. The collimating mirror (Figure 1) is a core component of the 4.51 keV beamline of the BEaTriX expanded X-ray beam facility; indeed, the optical quality of the mirror will directly affect the collimation and the uniformity of the final beam that will be used to characterize the focusing performance of SPO MM for ATHENA [RD2]. The mirror is made of HOQ 310 fused quartz, procured from Zeiss in a preliminary grinding and lapping state, and subsequently finished by a sequence of polishing at the Zeeko robotic machine installed at INAF-OAB [RD3]. Improvement of the mirror figure has been achieved across several runs of IBF process, using the dedicated facility [RD4] at INAF-OAB. At each polishing/figuring step, the mirror profile and surface roughness have been characterized using suitable metrology tools at MediaLario [RD5].



Figure 1: the paraboloidal mirror of BEaTriX in the IBF facility of INAF-OAB, prior to a figuring run of the surface. The broken or chipped parts are outside the optically-finished areas and will not be used in operation, or in tests at PANTER.

The current status of the mirror surface metrology is summarized in Section 2.2. In order to validate the performances predicted from metrology, a test campaign at the PANTER facility has been scheduled before and after the coating. After the first series of tests, a 30 nm-thick platinum layer will be deposited at DTU (plus a 4 nm chromium layer underneath platinum, in order to promote its stability [RD6]) to endow the mirror with reflective properties at 4.51 keV also. At 1.49 keV, in contrast, the bare mirror is reflective even without platinum coating.

The expected intrinsic angular resolution of this mirror is close to 2 arcsec, approx. the same angular width of the X-ray source in use at PANTER. Moreover, the low divergence of the X-ray beam at PANTER will induce an aberration twice as large [RD7]. For this reason, the zone plate (ZP) already available will be used to make the beam parallel, albeit at the expense of the beam intensity and the integration time required. The ZP works only at 1.49 keV, indeed at this stage the uncoated mirror will not be measured at 4.51 keV.

In this measurement campaign in the uncoated mirror, we are aiming at the following results:

- *measurement of the mirror focal length* with the source at infinity (i.e. the zone plate on) and the beam parallel to the mirror's optical axis (Sect. 3.1.2);
- *characterization of the focal spot* (PSF) at 1.49 keV with the parallel beam, in the best focus and alignment conditions (Sect. 3.1.3);
- *effective area measurement* (EA) at 1.49 keV in the same conditions;
- *intra-focal exposures* at 1.49 keV, for independent mirror shape diagnostic (Sect. 3.1.4).

After the coating deposition at DTU, the same measurement campaign at PANTER should be repeated, this time at both 1.49 keV and 4.51 keV, aiming at measuring the same quantities on the mirror (Sect. 4).

2. Preliminary analysis

2.1. Mirror geometry

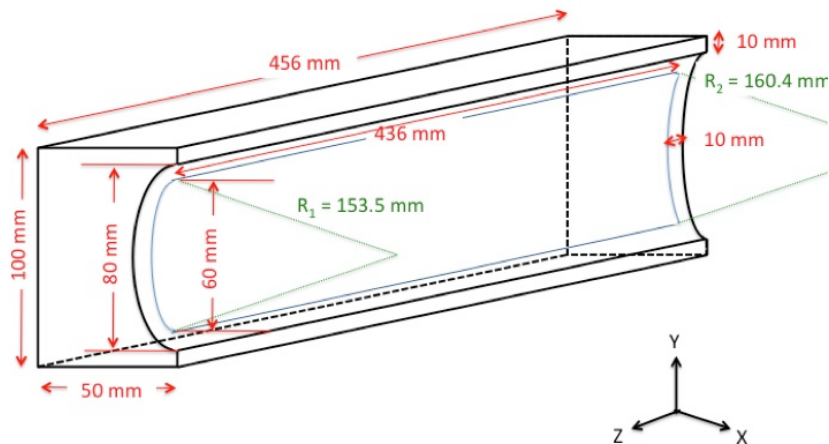


Figure 2: geometric parameters of the BEaTriX paraboloidal mirror. In the BEaTriX setup, the microfocuss source will be placed on the minimum diameter side, at approx. 4741 mm from the beginning of the optically-finished part, measured along the axis. In the PANTER setup, the full X-ray illumination comes from the max. diameter side, and will involve the central 400 mm × 60 mm area.

A drawing of the mirror with characteristic dimensions is displayed in Figure 2. More information not reported in the picture is listed hereafter:

- focal length along the axis: 4959 mm from the mirror center
- focal length along the rays: 4961 mm from the mirror center
- central RoC: 156.94 mm
- incidence angle at mirror center: $\alpha = 0.91$ deg
- meridional sag: 37 μ m

2.2. Mirror metrology

2.2.1. Mirror profile

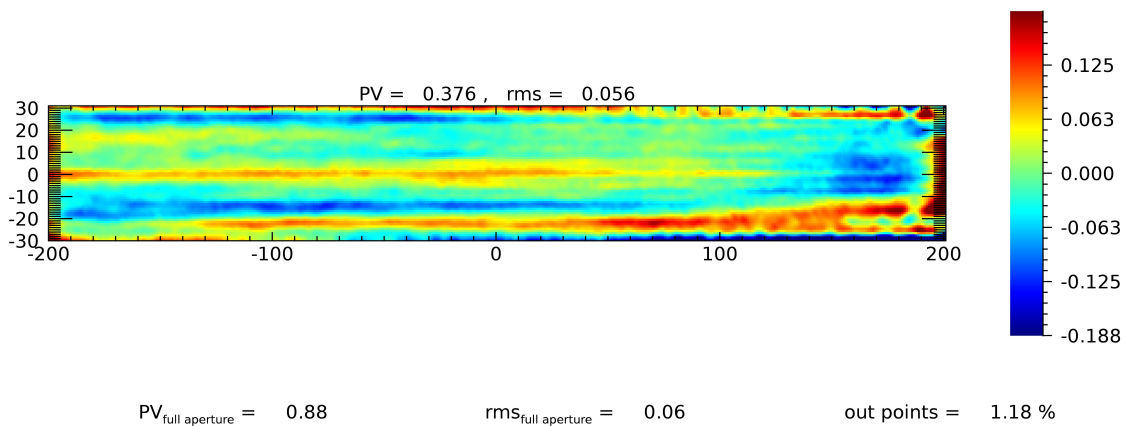




Figure 3: topographic map of the mirror shape error obtained by the MPR at Media-Lario [RD5]. The minimum diameter is on the right side.

 	Test plan of the BEaTriX paraboloidal mirror at PANTER				
Code: 02/2021	OAB Technical Report	Issue: 1	1	Class	Page: 6 / 18

We display in Figure 3 the error map of the mirror shape in its current status (after polishing run No. 38). The measurement has been taken at Media-Lario using the MPR metrology tool, properly adapted to detect the inner surface of a concave mirror. The residual defects have a 60 nm rms and are oriented in the axial direction, so to have a lesser impact on the focus degradation. A preliminary HEW estimate returned **2 arcsec**. Such a value would make the mirror suitable for installation in BEaTriX.

The MPR measurement did not return the sagittal RoC, which was measured with the CMM at OAB. It was not really simple having the MPR and CMM datasets match; therefore, some uncertainty still remains about the absolute RoC variation. They could, in fact, differ from the nominal ones by some 10 μm . This might add some astigmatism to the focal spot, but the related impact on the HEW should not exceed some 0.1 arcsec.

2.2.2. Mirror roughness

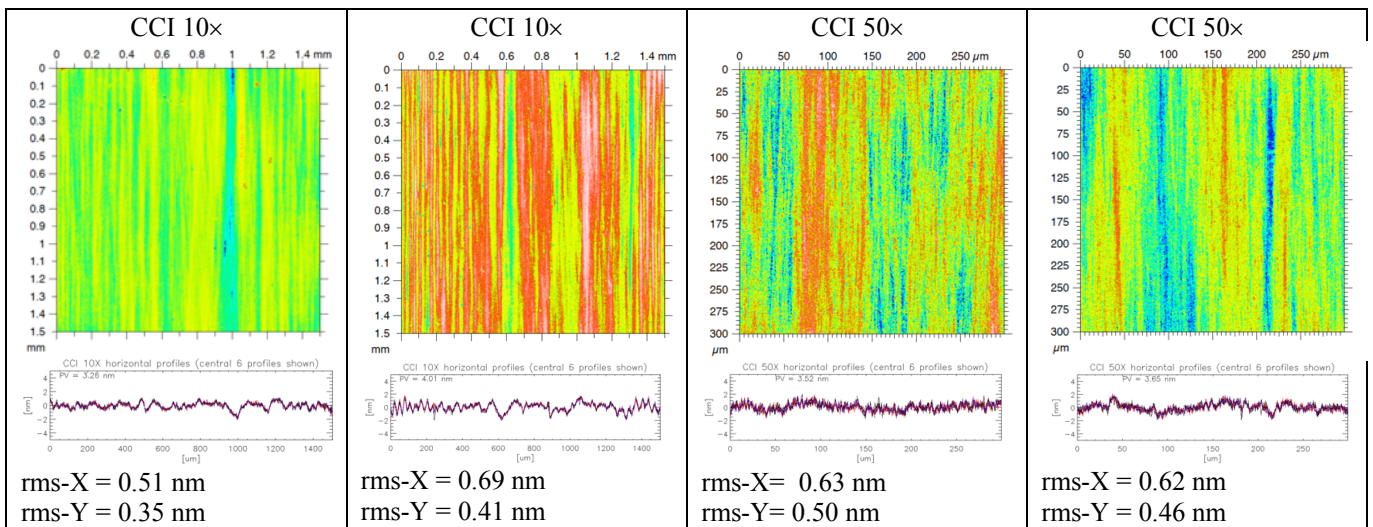


Figure 4: roughness measurements with CCI at Media-Lario, at two different magnifications, on the BEaTriX mirror. The optical axis of the paraboloid is oriented vertically. The grooved pattern is the result of the indentation caused by the abrasive particles used for the polishing process.

Surface roughness has been detected using the MFT instrument at OAB and the CCI instrument at Media-Lario, at different magnifications (2.5 \times , 10 \times , and 50 \times , see Figure 4). Several runs allowed us to damp the surface jaggedness to a level of 6 \AA rms. The residual marks of the polishing process are mostly oriented in the axial direction, therefore the roughness measured along the axis, (i.e., in the incidence plane of X-rays) is minimized.

The computation of the PSD along the axis and that of the related scattering diagram [RD8] allowed us to conclude that the contribution of the scattering to the HEW at 1.49 keV and 4.51 keV is less than 0.3 arcsec. Nevertheless, the roughness pattern is markedly anisotropic, which hardly makes 1D computations accurate. For this reason, we have computed approximate 2D diffraction pattern from the roughness maps themselves, following an FFT-based approach similar to the one described in [RD9]. This approach only considers the contribution of the roughness visible in the 10 \times images, which is expected to have the highest impact among the three. The simulation result at the two energies is shown in Figure 5: the pattern is clearly enhanced in the horizontal direction, orthogonal to the grooves. Additionally, a diffuse halo of scattered rays is visible around the diffraction pattern, especially at 4.51 keV. Nevertheless, the scattering impact on the mirror HEW is well below 0.2 arcsec, being dominated by the pixel size adopted in the simulation.

Finally, combining into a ray-tracing routine the information of topography and the computed scattering diagrams, we obtain the focus expected at 1.49 keV and 4.51 keV (Figure 6). The simulation assumes a 4 μm pixel on the detector, and an infinitesimal source at infinite distance.

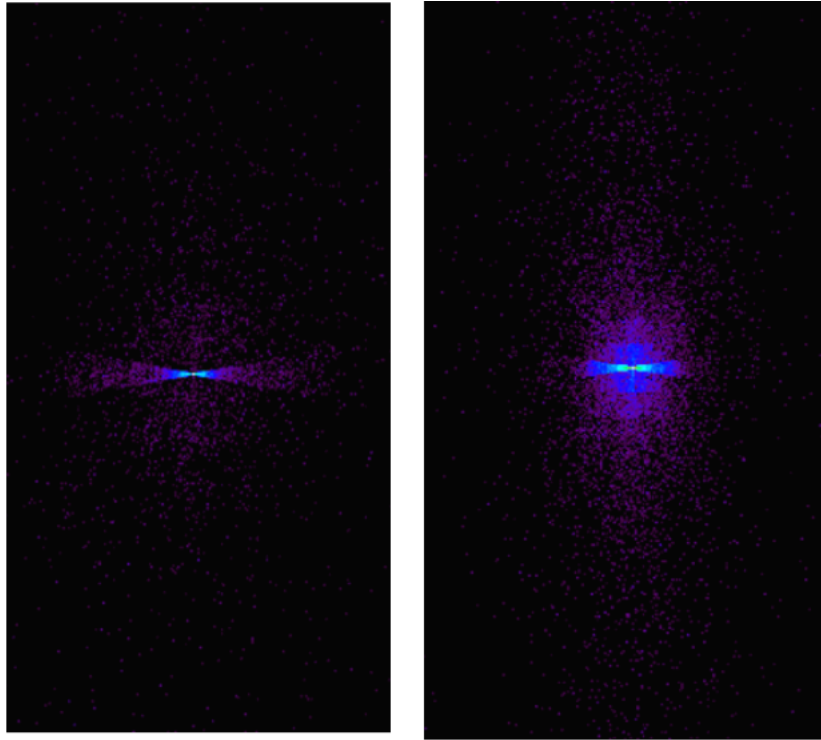


Figure 5: expected 2D scattering pattern (left) at 1.49 keV and (right) at 4.51 keV from the roughness measured with the CCI 10× (Figure 4), in logarithmic color scale. The image heights are approx. 1.5 mm. The HEW is 0.2 arcsec in both cases, entirely dominated by the pixel size. The W90 equals 0.5 arcsec at 1.49 keV and 3 arcsec at 4.51 keV.

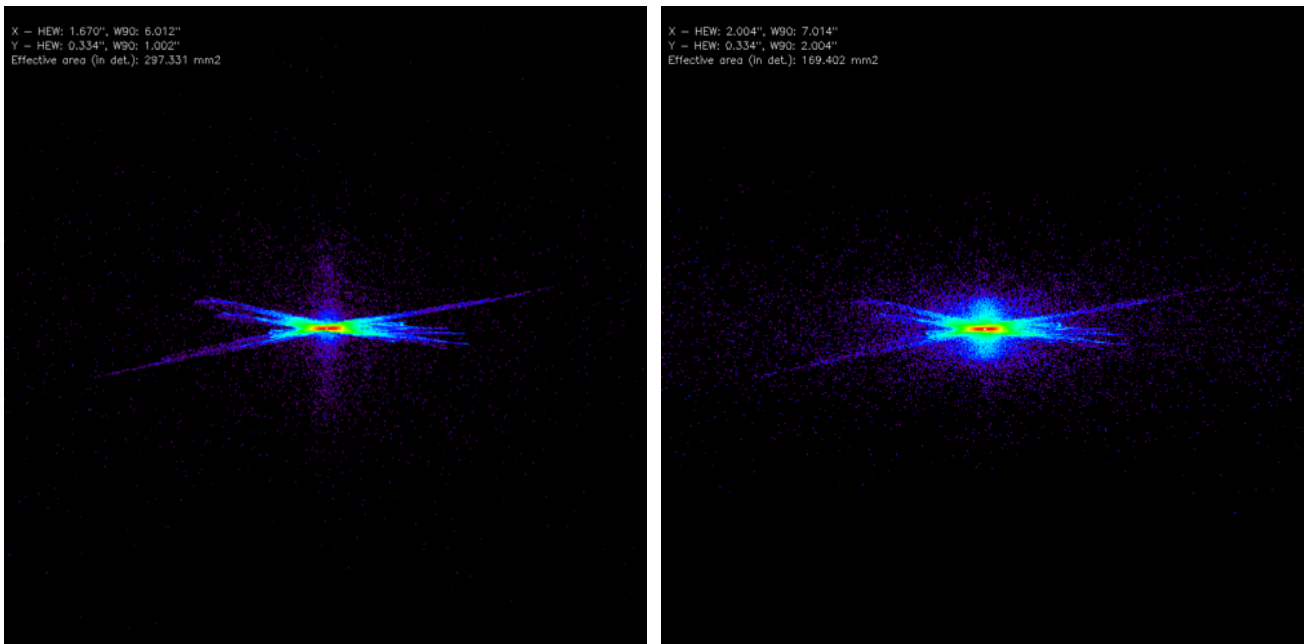


Figure 6: theoretical image in best focus, best align, and with illumination in perfectly-parallel X-rays, assuming a 4 μm -pixel spatial resolution. The frame size is 2 mm and the assumed pixel size is 4 μm . **Left: 1.49 keV, HEW = 1.8 arcsec. Right: 4.51 keV, HEW = 2 arcsec.** The color scale is logarithmic. Unlike Figure 4 (and from this point on) the horizontal direction lies in the meridional plane of the optic and the sagittal plane is vertical. The image orientation is the one of an observer staring at the X-ray source.

2.3. Mirror setup at PANTER

The mirror in PANTER will stand on the same kinematic supports used for the optical metrology and for the final configuration in BEaTriX: the kinematic pads were glued with vacuum compatible glue. The slit, defining the optical area to be illuminated in PANTER, has been aligned to the parabolic mirror with the 3D metrology equipment CMM. The slit design is shown in Figure 7. The slit is mounted at the phi-max side, towards the PANTER X-ray source. The slit is designed to ensure the illumination of the central longitudinal 400 mm, i.e., the sole optically-finished part, and manufactured in stainless steel with thickness 0.5 mm, sufficient to stop X-rays up to 4.5 keV.

The slit was aligned to the mirror, ensuring a maximum of 5 mm tolerance of illumination in the longitudinal direction, which is negligible compared to the 400 mm optical length. A picture of the mirror mounted on the PANTER support, along with the illumination slit, is shown in Figure 8, left.

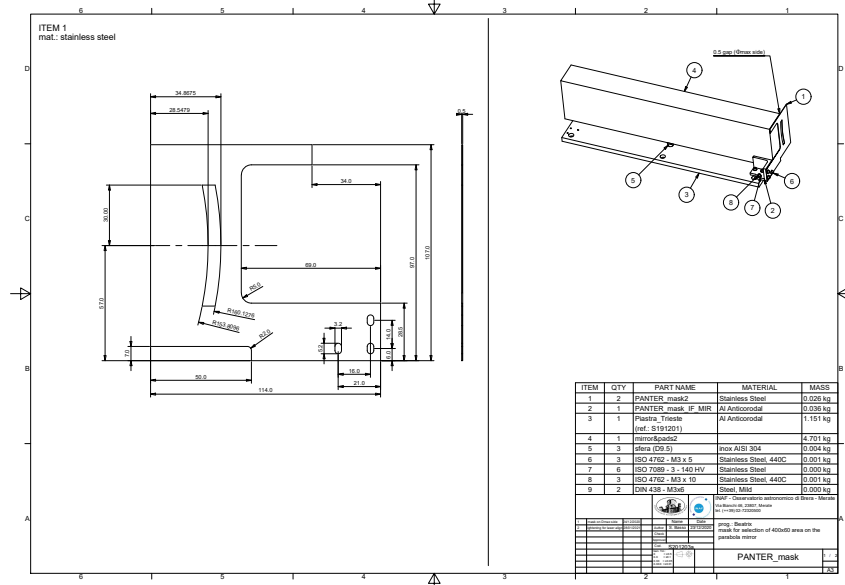


Figure 7: drawing of the slit placed in front of the mirror and interface plate.

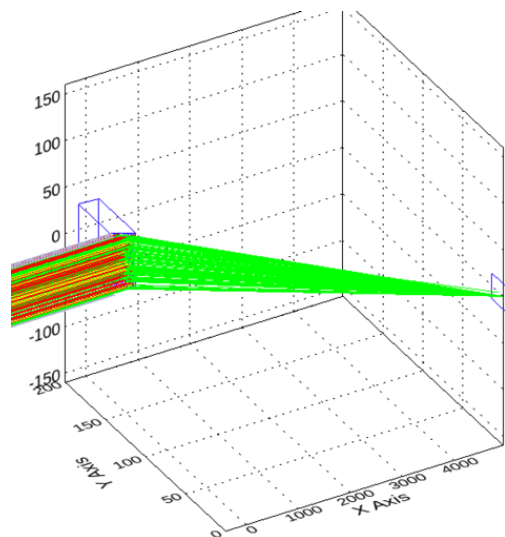
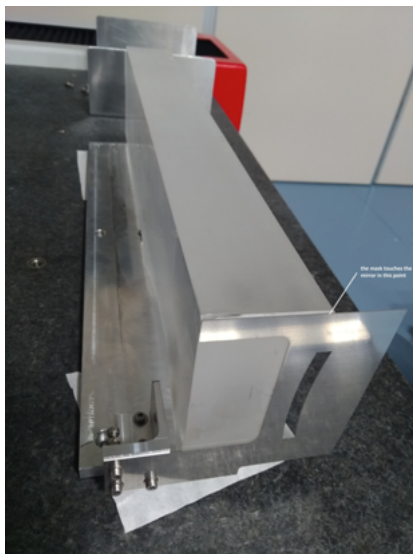




Figure 8: Left: the mirror on the supporting structure for PANTER, with the slit mounted at the maximum diameter. Right: ray-tracing model for the paraboloidal mirror. The PLXI detector is the rectangle on the right side, located on the optical axis. The oncoming beam is assumed at infinite distance. Red rays are absorbed, green rays are reflected.

 	Test plan of the BEaTriX paraboloidal mirror at PANTER				
Code: 02/2021	OAB Technical Report	Issue: 1	1	Class	Page: 9 / 18

Among the detectors available at PANTER, we suggest using PIXI for the highest possible spatial resolution ($20 \mu\text{m}$). The finite distance of the source has a small impact, but larger than the expected angular resolution of the mirror, even at the shifted best focus located 200 extra the nominal focal distance (i.e., 5159 mm from the mirror center, *measured along the axis*, 5161 mm *measured along the rays*). The exact distance may vary with the exact distance to the source. Even at the shifted focus, the divergence is expected to cause residual aberrations. The finite size of the source also contributes to significantly broaden the focal spot. If the BEaTriX paraboloid was perfect, for example, it would return a HEW value of 4.8 arcsec with the diverging beam and 1.6 arcsec with the parallel beam (see Figure 9; all the simulations will assume, from now on, a 125 m distance from the source to the mirror center). For this reason, we suggest using the zone plate (ZP) available at PANTER and operated at 1.49 keV, to make the beam parallel and so test the BEaTriX mirror to higher significance.

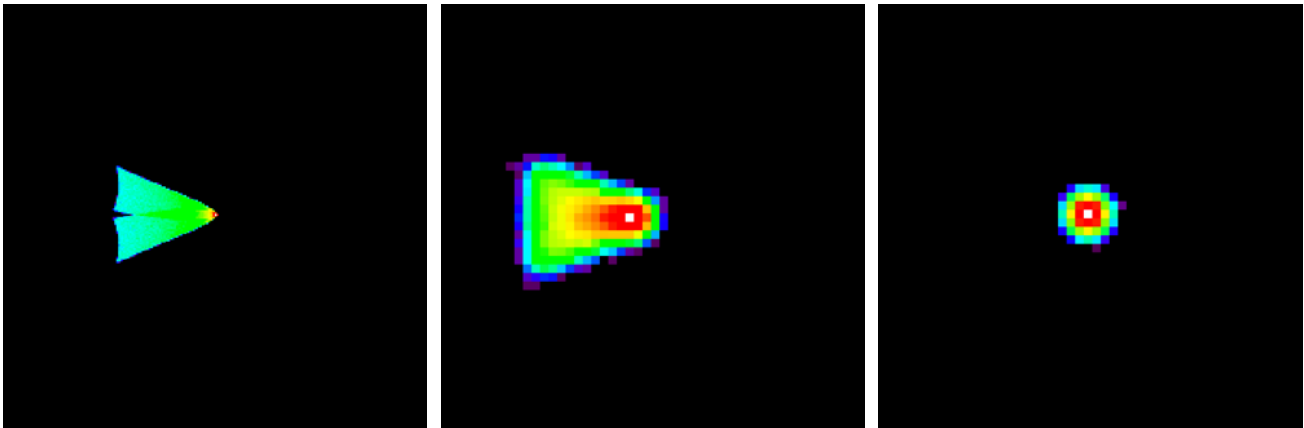


Figure 9: ray-tracing result for a perfect paraboloidal mirror, with the source at finite distance (123.8 m) at the best alignment and the best focus. The frame size is 1 mm. Left: without ZP, ideal case with a point-like X-ray source and $4 \mu\text{m}$ -wide pixels. Right: no ZP, 1 mm-FWHM Gaussian X-ray source and PIXI. Right: with the ZP and PIXI.

3. Test plan at PANTER, before coating

3.1. Tests in diverging beam at 1.49 keV

3.1.1. Initial alignment

After mounting of the parabola with his holder, an initial alignment can be achieved using the laser and the reference mirror fixed to the paraboloid bulk. In order to measure the absolute focal length of the mirror, we suggest that the distance from the PIXI sensor to the closest physical edge of the mirror surface be determined as precisely as possible, before closing the vacuum tank. *The expected distance is 4731 mm with the parallel beam and 4931 mm with the diverging beam.* This distance can be re-measured leaving the PIXI sensor in the best focus at the campaign end and re-measuring the distance before removing the parabolic mirror. The center of the travel range in the detector stage can be mounted at a 4831 mm distance from the closest edge of the parabola.

3.1.2. Alignment in X-rays and best focus search

The initial alignment in X-rays can be performed with the diverging X-ray beam. The mirror will hardly be in the best alignment and focus position when it is illuminated with X-rays for the first time. In order to find the best focus, we will have to act on three variables: the mirror yaw δ (in the vertical plane), the mirror pitch θ (in the horizontal plane), and the detector distance z from the best focus (as shifted by the diverging beam). The best alignment and focus are determined by $\delta = 0$, $\theta = 0$, $z = 0$. The yaw angle is positive when the optical axis is below the X-ray source. The pitch angle is positive when increasing the incidence angle. The